VOL. 11, NO. 19, OCTOBER 2016 ISSN 1819-6608
ARPN Journal of Engineering and Applied Sciences

www.arpnjournals.com

COMPARATIVE ANALYSIS AND SIMULATION OF INTEGRATED HALL ELEMENTS FORMED IN CMOS-TECHNOLOGY

Yury Goryachkin[1], Alexander Odnolko[2] and Mikhail Pavlyuk[2]
[1]Engineering Sciences, Department of Electronics and Nanoelectronics, National Research Mordovia State University, Saransk, Mordovia, Russian Federation
[2]Analog IC Design Department, JSC «ICC Milandr», Zelenograd, Moscow, Russian Federation
E-Mail: info@milandr.ru

ABSTRACT

The paper presents the results of a comparative analysis of X-FAB's technologies to obtain the most optimal parameters of drain current and the Hall voltage of the Hall element as a component of an integrated circuit with linear output formed in CMOS technology. It has simulated Hall elements in TCAD and found out that XH035 technology allows providing the most optimal parameters of drain current and the Hall voltage of the Hall element. Simulation results of the dependence of the Hall voltage on the width W of the Hall element at the length L = 200 μm have shown that the optimum ratio of the width W to the length L of the Hall element is within 1.25 <W/L <1.5. The paper has also simulated the dependence of the Hall voltage on the size of Hall contacts and shown that the most optimal size of Hall contacts in relation to the Hall voltage and required space is from 0 to 10 μm for L = 200 μm.

Keywords: hall element, CMOS technology, magnetic field, hall voltage, drain current, electric field, simulation.

1. INTRODUCTION

Recently, in modern microelectronics such sensors of physical quantities as temperature, pressure, acceleration, angle (tilt), rotation, and other ones have become widespread. The most important among them are magnetic field sensors.

Magnetic field-effect circuits with linear output where the Hall voltage is measured proportionally to the magnetic field induction are used to measure quite small magnetic field variations. As a rule, these circuits have a sensor amplifier. When no external magnetic field exists, the output voltage of a linear magnetic field-effect circuit taken for the reference level and usually equal to half of the supply voltage. When registering the positive direction of the magnetic field the output voltage is above the reference level, when registering the negative direction it is lower, although it remains a positive value [1].

2. STATEMENT OF THE PROBLEM

The main element of a magnetic field sensor is a magnetic field transducer. Hall elements are among the most well-known linear magnetic field transducers. Silicon (Si), gallium arsenide (GaAs), indium arsenide (InAs) and indium antimonide (InSb) are most widely used to make Hall elements. Hall elements made from GaAs, InAs and InSb possess high mobility of current carriers and allow to obtain the maximum Hall voltage. On exposure to the magnetic field with induction of 500 Gauss for Hall elements made from GaA the Hall voltage reaches 110 mV at the voltage of 6V. For Hall elements made from InAs the Hall voltage reaches 130 mV at the voltage of 3V. The maximum Hall voltage is reached for Hall elements made from InSb (up to 370 mV at the voltage of 1V) [2]. However, all these Hall elements are much more expensive than silicon Hall elements. Moreover, they are made in discrete implementation. Therefore the purpose of this study was to obtain the maximum Hall voltage for the Hall element implemented on silicon as a component of an integrated circuit.

The silicon Hall element can be implemented in standard processes of making integrated circuits such as bipolar or CMOS technologies. Hall elements made in CMOS technology possess high reliability, small size, low cost and are compatible with other CMOS elements [3-6]. Usually compatible CMOS Hall elements are formed in the n-type well.

Such the Hall element can be pinched from above by the p-type layer. Then it is actually a field-effect transistor or otherwise a pinch-resistor pinched on both sides by p-n junctions. Such the structure is less sensitive to charges on the silicon-oxide interface because it does not touch to oxide from any side and hence is not subject to the accumulated charge in oxide.

3. REVIEW OF X-FAB'S TECHNOLOGIES

X-FAB has more than a dozen of CMOS technologies with design rules from 0.18 to 1 μm. The analysis of these technologies has found that the development of such the Hall element suitable 4 special technologies such as XT018, XC06, XT06 and XH035. Table-1 presents the parameters of layers which can be used for the development of the Hall element are the layer resistance R_S and the depth x_j.

Table-1. The parameters of layers.

Technology	Layer	R_S, Ohm/sq.	x_j, µm
XT018	nWell	1080 (below STI)	1.5
	p+	135	0.2
	n+	62	0.2
	STI		0.4
XC06	SnWell	1800	6
	pWell	2000	3
	p+	115	0.4
	n+	57	0.6
XT06	SnWell	1500	5
	pWell	750	3
	p+	115	0.4
	n+	57	0.6
XH035	deep nWell	2800	3.8
	pWell	5800	0.8
	p+	90	0.21
	n+	85	0.17

Moreover, there is XI10-technology which has the finished Hall element. Its structure is the active n-type layer with the layer resistance R_S of 4500 Ohm/sq. and thickness of 0.25 µm located on the concealed oxide layer (BOX) thickness of 1 µm. The active layer resistance is 6.9 kOhm. Current I through the Hall element is 300 µA at the same time the sensitivity S is 205 V/A·T. However, the range of magnetic fields is only from 200 to 2000 Gauss. Thus, the Hall voltage V_H when the magnetic field induction B is 200 Gauss will be only $S\,I\,B$ = 1.2 mV. Besides, the calculation shows that the Hall element operating voltage is only 2V and is limited by the linear range of current-voltage characteristic. Higher voltage will lead to channel closure.

Thus, the maximum Hall voltage demands low impurity concentration in the active layer to achieve maximum mobility and high thickness of the active layer to avoid channel closure. Therefore, the paper further has conducted a selection of processes to contain the specified Hall element which will allow to obtain the maximum Hall voltage. For this purpose the paper has conducted the study by simulation in TCAD.

Figure-1 schematically shows configurations and structures of Hall elements at section 1 for XT018, XC06, XT06 and XH035 technologies. L and W - are respectively the length and width of the Hall element (actually the channel length and width), S – is a source region, D – is a drain region, G – is a gate region, HL and HR – are Hall contacts, STI and BOX - are dielectric insulating layers, FOX – is field oxide.

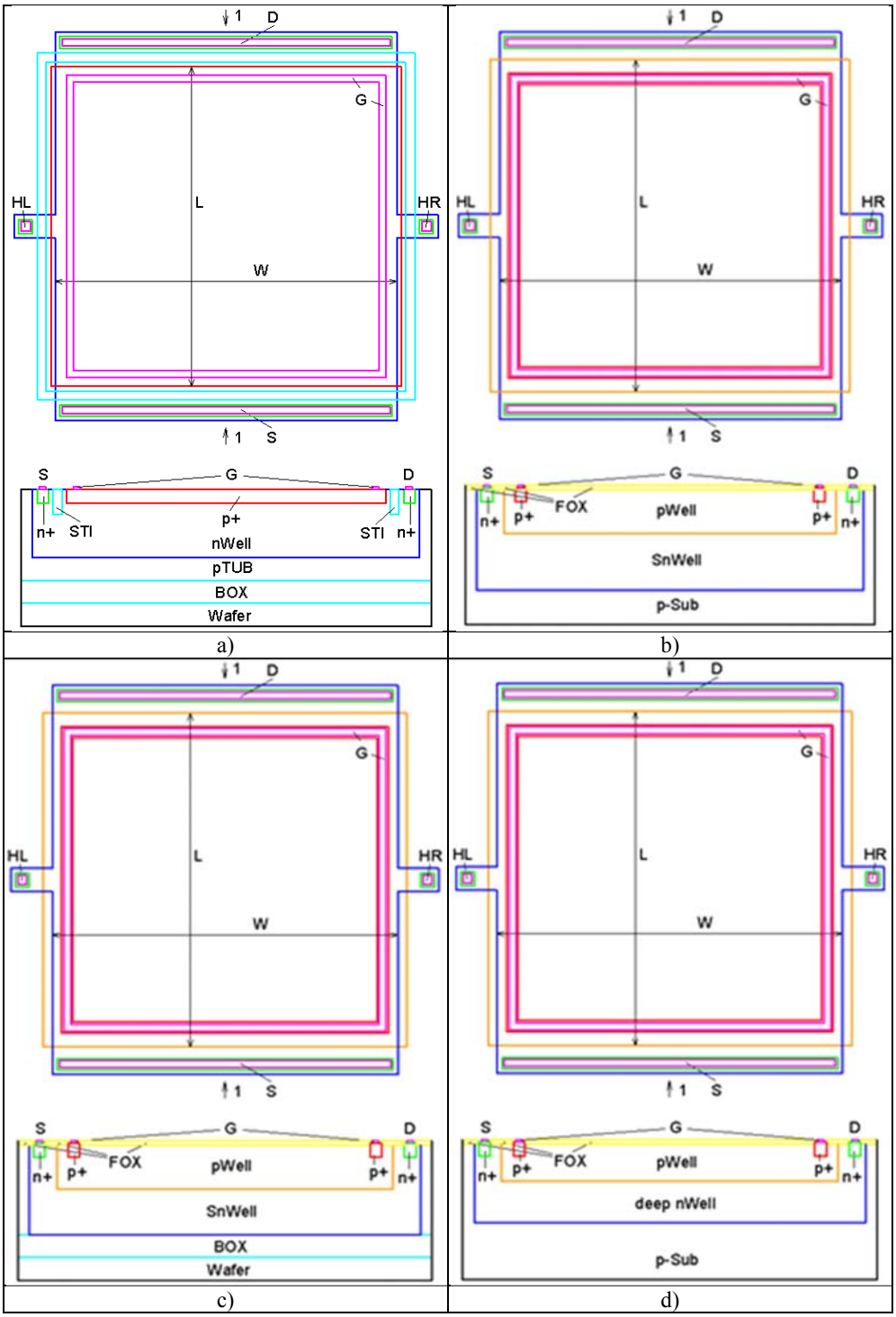

Figure-1. Configurations and structures of Hall elements for XT018 (a), XC06 (b), XT06 (c) and XH035 (d) technologies.

4. DEVELOPMENT OF HALL ELEMENT MODELS

Models of three-dimensional Hall elements' structures formed on the above mentioned X-FAB's techniques were created to simulate in TCAD. As TCAD can specify the contact resistance (arbitrarily small), n+ layers around source, drain and Hall contacts and p+ layers around gate contacts were not created for simplicity. STI, BOX and FOX layers were also not made.

Figure-2, a shows a part of the Hall element three-dimensional structure on contacts to a drain / source side, Figure-2, b on Hall contacts side, for XT018 technology. XC06, XT06 and XH035 technologies are

only distinguished by concentrations and depth of layers. Figure-3 shows impurity distribution profiles in simulated Hall elements' structures for XT018, XC06, XT06 and XH035 technologies.

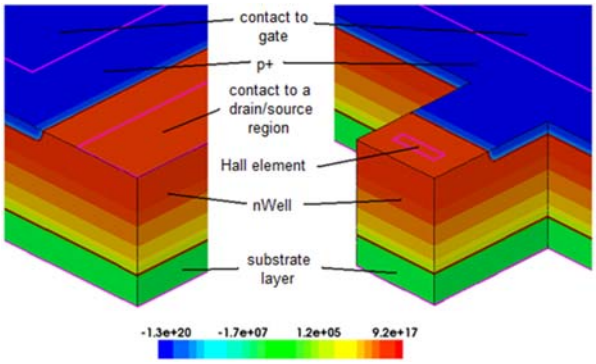

a) b)

Figure-2. Part of the Hall element structure from contacts to a drain / source region (a) and from Hall contacts (b).

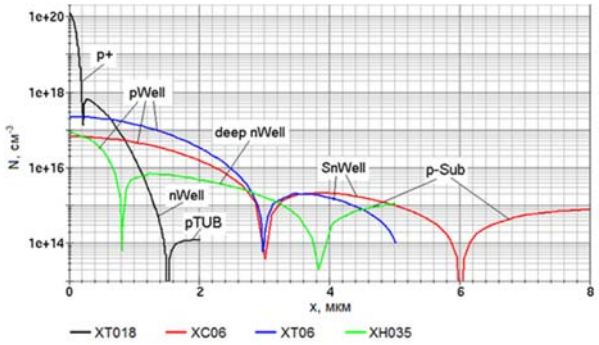

Figure-3. Impurity distribution profiles in the Hall element structure.

Table-2 presents parameters of Hall elements' modeled structures: surface impurity concentration in the active n-type layer below the p-type layer N_{Sa}, mobility of current carriers μ at the pointed value of surface concentration thickness of the active layer h.

Table-2. The parameters of Hall elements.

Technology	N_{Sa}, cm^{-3}	μ, cm^2/V·s	h, µm
XT018	$6 \cdot 10^{17}$	330	1.3
XC06	$2 \cdot 10^{15}$	1330	3
XT06	$2 \cdot 10^{15}$	1330	2
XH035	$7 \cdot 10^{15}$	1270	3

In simulation of Hall elements the drift-diffusion model was used and the following physical effects were taken into account:

- band gap width narrowing with increasing dopant impurity concentration;
- scattering of current carriers on phonons and charged impurity ions and saturation of the charge drift velocity in high fields;
- Shockley-Read-Hall recombination with current carrier lifetimes depending on dopant impurity concentration and also Auger recombination;
- the model of carrier galvanic transfer in magnetic fields.

Detailed description of these effects is given in [7].

5. SIMULATION OF HALL ELEMENTS

When simulating the width W of Hall elements varied from 100 and 300 µm at a 50µm-interval. The length of Hall elements L was equal to 200 µm. Figure-4 and Figure-5 show the simulation results of the dependence of drain current I_D and the Hall voltage V_H on the Hall element width at the Hall element length L of 200 µm on exposure to the magnetic field with induction of 640 Gauss and the voltage V_D of 5V between drain and source regions.

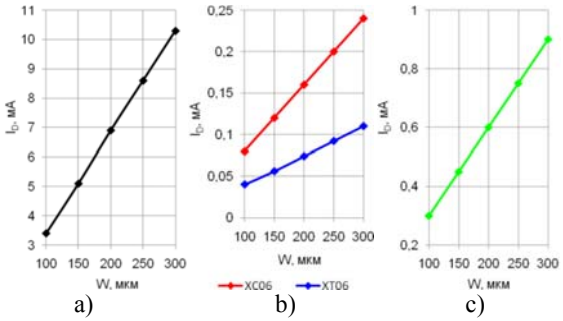

a) b) c)

Figure-4. Diagrams of the dependence of drain current on the Hall element width at the Hall element length L of 200 µm for XT018 (a), XC06 and XT06 (b) and XH035 (c) technologies.

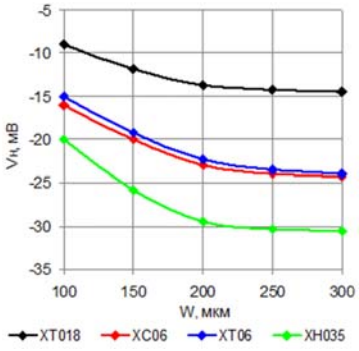

Figure-5. Diagrams of the dependence of the Hall voltage (b) of the Hall element width at the Hall element length L of 200 µm.

As the diagram in Figure-4 shows, the dependence of drain current on the Hall element width for all four analyzed technologies is linear, but the absolute current values greatly vary. At equal values of the Hall element width maximum drain current is for XT018

process and exceeds current for XH035 technology by 11 times, for XC06 process and for XT06 process by 43 and 94 times respectively.

Diagrams in Figure-5 show that the dependence of the Hall voltage on the Hall element width for all four processes is nonlinear and at $W/L > 1.25$ there is saturation. At that for XH035 process the Hall voltage exceeds by two times the Hall voltage for XT018 process and almost by one third for XC06 and XT06 processes at equal values of the Hall element width.

Hall elements of rectangular configuration are characterized by this dependence of the Hall voltage on the width which is explained by field curvature because of the large W/L and considered by the introduction of the well-known formula of a geometric factor which is included into the expression for the Hall voltage [8]:

$$V_H = G\mu_H VB\frac{W}{L} \quad (1)$$

where:
G - is a geometric factor ($0 < G \leq 1$)
μ_H - is Hall mobility,
V - is the applied voltage (in this case between drain and source regions of V_D),
B – is the incoming magnetic field induction.

Figure-6 presents current-voltage characteristic simulation results of Hall elements. For XT018 process the current-voltage characteristic linear range is about 9V and then almost instantly the p-n junction breakdown takes place. For XC06 and XT06 processes the linear current-voltage characteristic range is about 3V and then the channel closure in the active layer takes place. For XH035 process the linear current-voltage characteristic range is much greater and is about 8V and then the channel closure in the active layer also takes place. That means that the Hall voltage will not increase for XT06 and XC06 processes at the drain region voltage of more than 4V, and for XH035 process at the drain voltage of more than 10V.

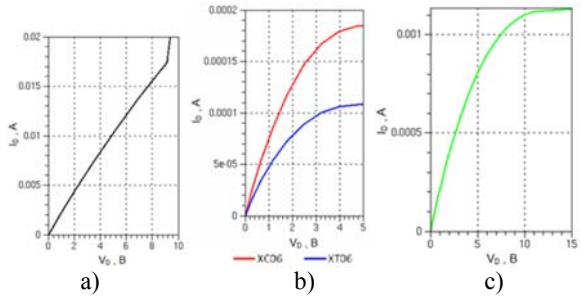

a) b) c)

Figure-6. BAX of Hall elements at the width W of 300 µm and the length L of 200 µm for XT018 (a), XC06 and XT06 (b) and XH035 (c) technologies.

The calculation of sensitivity of Hall elements which are subject to the magnetic field with induction of 640 Gauss and to the voltage V_D between drain and source regions of 5V at L = 200 µm and W = 300 µm shows that sensitivity S for XT018 process is 22 V/A·T, for XC06 2080 V/A·T, for XT06 3270 V/A·T and for XH035 605 V/A·T. As the calculations show that the Hall element manufactured in XT06 process has maximum sensitivity. However, a set of parameters allows making a conclusion that XH035 process will provide the most optimal parameters of the Hall element. Hall elements made in this process will have maximum Hall voltage (31 mV at the magnetic field induction of 640 Gauss), small current (less than 1mA), operating voltage range of up to 8V. Therefore, further simulation was conducted for this particular Hall element.

The minimum magnetic field value influencing the Hall element depends on the amplifier gain factor and is limited by noise. Noise at 100°C and the amplifier gain factor of 300, made in bipolar process, is about 15 mV, and made in CMOS process, is about 100 mV. These data were obtained in CAD Cadence simulation at the voltage V_D between drain and sources of 5V. The calculation shows that the minimum magnetic field value for bipolar process is 0.9 Gauss, for CMOS process is 6 Gauss.

Further the paper has considered how the Hall voltage on the Hall element volume changes. For this purpose, the paper has developed and simulated Hall elements' structures of different width which include contacts inside the Hall element located between left and right Hall contacts HL and HR in the equal distance from each other as Figure-7 shows.

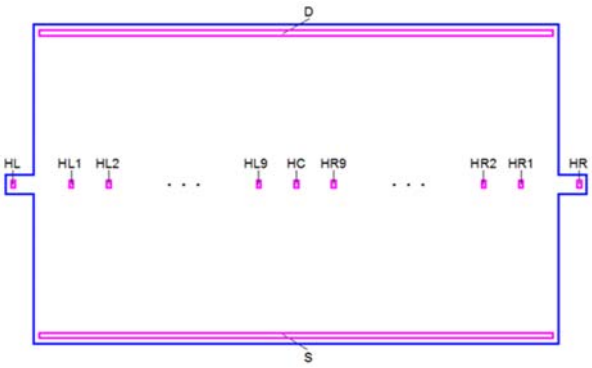

Figure-7. The Hall element configuration with contacts inside the Hall element.

Here, the pWell layer is not developed, otherwise the number of elements of the computational grid becomes excessively large. The Hall element length L is 200 µm. HL and HR - are Hall contacts, HC – is a contact in the Hall element center, contacts HL1, HL2, ..., HL9 and HR1, HR2, ..., HR9 are located at the equal distance relative to the central HC contact. The Hall voltage was measured on these contact pairs (the left HLn and its corresponding right HRn, where n = 1, 2, ..., 9). As a result, the paper has constructed the graphs of the dependence of the Hall voltage V_H on these contact pairs on the distance ΔW measured from the left Hall contact HL (or the right HR) towards the center of the structure at

different values of the Hall element width *W*. Figure-8 shows these graphs. The first ten markers on these graphs, starting from the value $\Delta W = 0$ µm, correspond to the Hall voltage V_H measured on these contact pairs (HLn and HRn), starting from HL and HR Hall contacts. The last one, the eleventh marker corresponds to the voltage at the center contact HC which has the Hall voltage V_H of 0V.

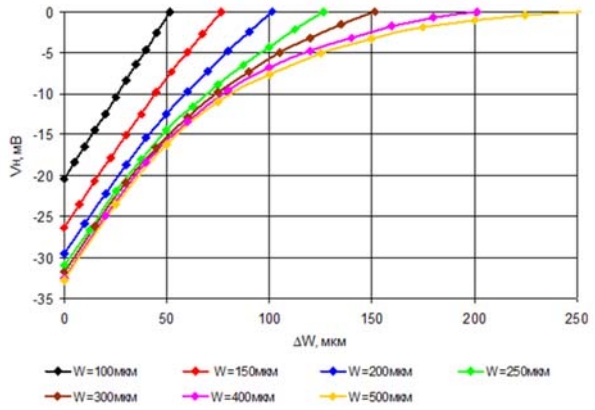

Figure-8. Diagrams of the Hall voltage dependence on corresponding contact pairs (HLn and HRn) on the distance measured from the left Hall contact HL (or the right HR) towards the center of the structure atdifferent values of the Hall element width.

These graphs show that for W = 100 µm the dependence is almost linear, namely, the transverse electric field is proportionally distributed throughout the Hall element. At W = 150 µm linearity is already broken and the small saturation closer to the Hall element center takes place. And then with increasing W the dependence saturation occurs in the increasing distance from the Hall element center. Starting from the value W = 250 ÷ 300 µm, the dependence linearity is kept only at the distance of 50 µm from the Hall element edges and then towards the center the dependence becomes much more nonlinear. At that the Hall voltage on Hall contacts HL and HR almost stops to increase. Consequently, a transverse component of the electric field is proportionally distributed in the distance of only 50 µm from the Hall element edges, but then towards the center it is reduced.

The paper has further researched the dependence of the Hall voltage on the length of Hall contacts *b* and on the length of the required space for Hall contacts *a* of the Hall element. Figure-9 fixes these distances. In this case, the Hall element length *L* is 200 µm and width *W* is 300 µm.

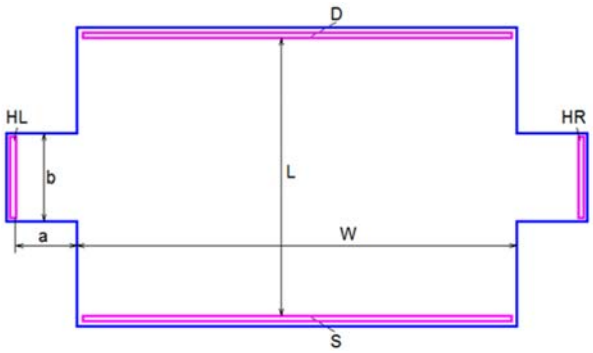

Figure-9. Structure of the Hall element for the research of the dependence of the Hall voltage on the length of Hall contacts and the length of the required space for Hall contacts of the Hall element.

Figure-10 shows the graphs of the Hall voltage dependence on the ratio *a/b* at different values of the length of Hall contacts. The graphs show that with increasing length of Hall contacts the length of the space for Hall contacts at which the Hall voltage reaches its maximum also increases. And the maximum value of the Hall voltage does not depend on the length of Hall contacts and is 31 mV.

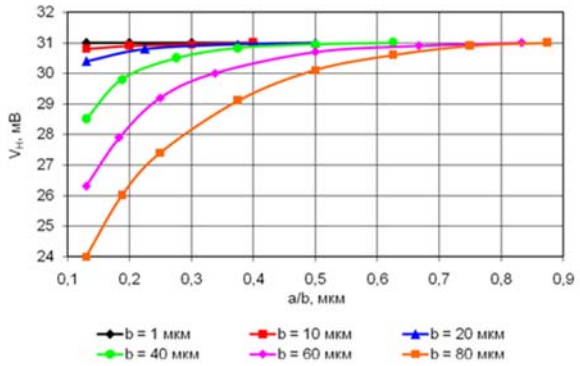

Figure-10. Diagrams of the Hall voltage on the ratio a/b for different values of the length of Hall contacts.

According to simulation data, test Hall elements will be developed and manufactured. Results of the study will be published in the next paper.

6. CONCLUSIONS

Thus, the results of the Hall element simulation allow to make the following conclusions:

a) Comparative analysis of X-FAB's processes shows that XH035 process provides the most optimal parameters of drain current and the Hall element voltage.

b) Results of Hall elements' simulation in TCAD have shown that the optimal ratio of the width *W* to the length *L* of the Hall element is within $1.25 < W/L < 1.5$.

c) Also simulation results have shown that the optimal size of Hall contacts in relation to the Hall voltage and required space is from 0 to 10 μm for L = 200 μm.

ACKNOWLEDGEMENT

The study was supported by the Ministry of Education and Science of the Russian Federation (Agreement № 14.576.21.0026 from 30 June 2014, unique identifier PNI RFMEFI57614X0026).

REFERENCES

[1] Ageev O.A., Mamikonova V.M., Petrov V.V., Kotov V.N. Negodenko O.N. 2000. Microelectronic transducers of nonelectric quantities. - Taganrog: Taganrog State University of Radio Engineering Publishing House. p. 153.

[2] Hall Elements, http://www.akm.com/akm/en/product/detail/0004.

[3] Bellekom S. 1999. CMOS versus bipolar Hall plates regarding offset correction. // Sens. Actuat. A. (76): 178-182.

[4] Blanchard H., De M.F., Hu B.J., Popovic R.S. 2000. Highly sensitive Hall sensor in CMOS technology. Sens. Actuat. A. (82): 144-148.

[5] Popovic R.S., Randjelovic Z., Manic D. 2001. Integrated Hall-effect magnetic sensors. Sens. Actuat. A. (91): 46-50.

[6] Randjelovic Z.B., Kayal M., Popovic R., Blanchard H. 2002. High sensitive Hall magnetic sensor Microsystem in CMOS technology. IEEE Journal of Solid-State Circuits. (37): 151-158.

[7] Goryachkin Yu.V., Nesterov S.A., Surin B.P. 2006. Physicotopological simulation in CAD TCAD. - Saransk: Mordovia University Publishing House. p. 124.

[8] Popovic R.S. 2004. Hall Effect Devices. - Bristol and Philadelphia: Institute of Physics Publishing. p. 426.